GEOPHYSICS, VOL. 66, NO. 3 (MAY-JUNE 2001); P. 904–910, 7 FIGS., 3 TABLES.

Velocity analysis for tilted transversely isotropic media: A physical modeling example

Vladimir Grechka*, Andres Pech*, Ilya Tsvankin*, and Baoniu Han*

ABSTRACT

Transverse isotropy with a tilted symmetry axis (TTI media) has been recognized as a common feature of shale formations in overthrust areas, such as the Canadian Foothills. Since TTI layers cause serious problems in conventional imaging, it is important to be able to reconstruct the velocity model suitable for anisotropic depth migration. Here, we discuss the results of anisotropic parameter estimation on a physical-modeling data set. The model represents a simplified version of a typical overthrust section from the Alberta Foothills, with a horizontal reflector overlaid by a bending transversely isotropic layer.

Assuming that the TTI layer is homogeneous and the symmetry axis stays perpendicular to its boundaries, we invert P-wave normal-moveout (NMO) velocities and zero-offset traveltimes for the symmetry-direction velocity V_0 and the anisotropic parameters ϵ and δ. The coefficient ϵ is obtained using the traveltimes of a wave that crosses a dipping TTI block and reflects from the bottom of the model. The inversion for ϵ is based on analytic expressions for NMO velocity in media with intermediate dipping interfaces. Our estimates of both anisotropic coefficients are close to their actual values. The errors in the inversion, which are associated primarily with the uncertainties in picking the NMO velocities and traveltimes, can be reduced by a straighforward modification of the acquisition geometry. It should be emphasized that the moveout inversion also gives an accurate estimate of the thickness of the TTI layer, thus reconstructing the correct depth scale of the section.

Although the physical model used here was relatively simple, our results demonstrate the principal feasibility of anisotropic velocity analysis and imaging in overthrust areas. The main problems in anisotropic processing for TTI models are likely to be caused by the lateral variation of the velocity field and overall structural complexity.

INTRODUCTION

Transverse isotropy (TI) is one of the most common anisotropic models encountered in the subsurface. The main physical reasons for the TI (or hexagonal) symmetry are the intrinsic anisotropy of sedimentary formations (primarily shales) and periodic fine layering. Horizontally layered sediments are characterized by TI media with a vertical symmetry axis (VTI). In active tectonic areas, however, anisotropic layers (or interbedding isotropic sediments) may be dipping, thus giving rise to TI media with a tilted axis of symmetry (called here TTI). For example, uptilted shale layers near salt domes are expected to produce an effective TTI medium with a large inclination of the symmetry axis. The TTI model should also be rather typical for overthrust areas, such as the Canadian Foothills, where TI shale layers are often bent by tectonic processes and may have dips exceeding 45° (e.g., Leslie and Lawton, 1996).

The presence of TTI formations in overthrust areas may cause serious problems in imaging of exploration targets. Ignoring the influence of transverse isotropy and applying conventional (isotropic) velocity-analysis and migration techniques leads to mispositioning of reflectors beneath TTI layers and inferior quality of seismic sections (Leslie and Lawton, 1998; Isaac and Lawton, 1999). Leslie and Lawton (1998) and Vestrum et al. (1999) showed on model and field data that higher-quality images of both dipping and horizontal features in the overthrust environment are produced by migration algorithms capable of handling TTI media. The main difficulty, however, is in evaluating the anisotropic parameters from surface reflection data, especially in structurally complex areas.

Although the physical reasons leading to TI models with a vertical and tilted symmetry axis are similar (e.g., Levin, 1979), the parameter-estimation problem for TTI media is

Manuscript received by the Editor June 7, 1999; revised manuscript received April 12, 2000.
*Colorado School of Mines, Center for Wave Phenomena, Dept. of Geophysics, 13th and Maple, Golden, Colorado 80401. E-mail: vgrechka@ka@dix.mines.edu; apech@dix.mines.edu; ilya@dix.mines.edu; bhan@dix.mines.edu.

much more involved, even if the tilt is assumed to be known. Time processing of P-waves in models with a vertically inhomogeneous VTI overburden is controlled by the interval values of just two parameters—the NMO velocity from a horizontal reflector ($V_{\rm nmo}$) and the "anellipticity" parameter η (Alkhalifah and Tsvankin, 1995). Both $V_{\rm nmo}$ and η can be obtained from P-wave reflection traveltimes acquired in the dip direction of the structure using either the normal-moveout (NMO) velocity of dipping events or nonhyperbolic (long-spread) moveout.

These results, however, do not hold in TTI media where, in general, the velocity-analysis problem has to be treated in three dimensions. P-wave kinematics in TTI media is controlled by the dip and azimuth of the symmetry axis, symmetry-direction P-wave velocity V_0, and Thomsen's (1986) anisotropic coefficients ϵ and δ (Tsvankin, 1996, 1997). As shown by Grechka and Tsvankin (2000), if the tilt of the symmetry axis exceeds 30°–40°, all these parameters can be found from P-wave traveltime data by inverting azimuthally dependent NMO velocities (i.e., NMO ellipses) of horizontal and dipping events. Therefore, in contrast to VTI media, P-wave reflection data constrain the depth scale of TTI media and can be used to build models for depth imaging. The methodology of Grechka and Tsvankin (2000), however, is limited to horizontally layered TTI models above a dipping reflector and requires wide-azimuth 3-D acquisition.

For P-wave data recorded on a single line in the dip direction of the reflector(s), the inversion for the TTI parameters is generally nonunique (Tsvankin, 1997). In the important special case of the symmetry axis orthogonal to the bottom of a homogeneous TTI layer, the NMO velocities of horizontal and dipping P events yield the tilt of the axis, the velocity V_0, and the parameter δ, but the anisotropic coefficient ϵ remains undetermined (Grechka and Tsvankin, 2000). Furthermore, the homogeneous model appears to be too simplistic for overthrust areas where tilts of the symmetry axis are associated with significant structural dips and lateral heterogeneity. However, while in general lateral heterogeneity causes nonuniqueness in anisotropic inversion, the presence of intermediate dipping interfaces may actually help to resolve some of the trade-offs between the model parameters (Grechka and Tsvankin, 1999). As demonstrated by Le Stunff et al. (2001), P-wave reflection traveltimes in a two-layer VTI model with a dipping intermediate interface may constrain the vertical velocities and, therefore, the depths of the reflectors.

Here, we arrive at a similar conclusion for a physical model that contains a bending TI layer with the symmetry axis orthogonal to the layer boundaries. The model was built by Leslie and Lawton (1996) to simulate typical reflection data acquired in overthrust areas of the Alberta Foothills in Canada. Using the general theory of normal moveout in laterally heterogeneous media developed by Grechka and Tsvankin (1999), we show that P-wave NMO velocities and zero-offset traveltimes measured on top of the model can be inverted for the full set of the anisotropic parameters of the TTI layer.

PHYSICAL MODELING

A 2-D physical model built at the University of Calgary by Leslie and Lawton (1996) was designed to imitate overthrust structures typical for the Central Alberta Foothills in Canada (Figure 1). Four blocks of Phenolic laminate (shaded in gray in Figure 1) were glued together to make up a bending TI layer with the symmetry axis orthogonal to the layer boundaries. The Phenolic material, which is known to be orthorhombic, was cut in the direction of one of the symmetry planes to produce a 2-D TI sheet with the parameters believed to be typical for shales in the Foothills. The P-wave velocities in the symmetry direction ($V_0 = 2925$ m/s) and isotropy plane ($V_{90} = 3365$ m/s) yield the anisotropic parameter $\epsilon = 0.16$, while the second relevant anisotropic coefficient, δ, is equal to 0.08 (Cheadle et al., 1991). The TI layer was embedded in a purely isotropic plexiglass material (white in Figure 1) with the P-wave velocity $V_{\rm iso} = 2740$ m/s.

Leslie and Lawton (1996) acquired an ultrasonic P-wave reflection survey at the top of the model; the acquisition parameters are given in Table 1. The time section for the smallest offset in the data (Figure 2) shows a false anticline structure at a time of approximately 1.4 s. This pull-up of the bottom of the model is caused by the combined influence of the higher velocity and anisotropy in the Phenolic blocks. Leslie and Lawton (1998) presented a series of prestack depth migrations of these data and showed that the bottom interface cannot be flattened without taking anisotropy into account. Their results also suggest that P-wave reflection traveltimes might contain sufficient information for obtaining the model parameters needed for the anisotropic imaging. Here, we use the theoretical results of Grechka and Tsvankin (1999) to perform a parameter-estimation procedure based on surface P-wave data.

PARAMETER ESTIMATION

Assumptions about the model

We begin by formulating the assumptions needed to avoid ambiguities in the inversion of the available set of measurements for the model parameters.

Table 1. Acquisition parameters used by Leslie and Lawton (1996).

Parameter	Value
Number of common midpoints	504
CMP spacing	10 m
Offset spacing	20 m
Minimum offset	200 m
Maximum offset	2000 m

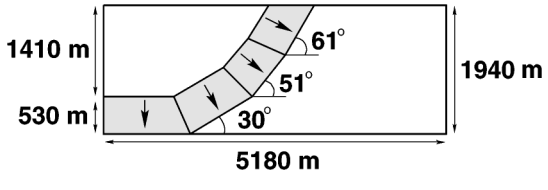

FIG. 1. Physical model of an anisotropic thrust sheet (after Leslie and Lawton, 1996). In each block of the bending TI layer, the symmetry axis (marked by the arrows) is perpendicular to the layer boundaries. The distances were scaled by a factor of 10 000.

1) All blocks making up the model in Figure 1 are assumed to be *homogeneous*. Allowing for lateral velocity variation leads to trade-offs between the parameters, such as those described for VTI media by Grechka (1998).
2) The four TTI blocks are made of the same material with the symmetry axis *orthogonal* to the bedding within each block. In other words, we have to assume that the model contains a homogeneous, bending TTI layer. Without this assumption, the number of independent parameters cannot be reduced to that constrained by the data.
3) The Plexiglass blocks (white in Figure 1) are *isotropic*. This assumption is difficult to verify using the available data because the same *P*-wave reflection traveltimes from the top of the TTI layer could have been generated for an *elliptically anisotropic* overburden with the same value of the NMO velocity from horizontal reflectors (e.g., Alkhalifah and Tsvankin, 1995).
4) The reflector at the bottom of the model is *horizontal*, which implies that the anticline structure at approximately 1.4 s in Figure 2 is the result of the spatial velocity variations in the overburden. This assumption, which might be difficult to use in field-data applications, would not be needed if we could measure the NMO velocity for the reflection event marked as Ra in Figures 2 and 3 (see a more detailed discussion below).

Inversion for the anisotropic parameters

Under the above assumptions, it is possible to obtain all model parameters in the depth domain using the zero-offset traveltimes and normal-moveout velocities of reflection events R1–R5 marked in Figures 2–4. We also attempted to process reflections Ra and Rb, which carry information about the parameters of the TTI layer. However, the NMO velocities and zero-offset traveltimes of these events could not be picked with sufficient accuracy. The inversion procedure is described in detail below, and the results are summarized in Tables 2 and 3.

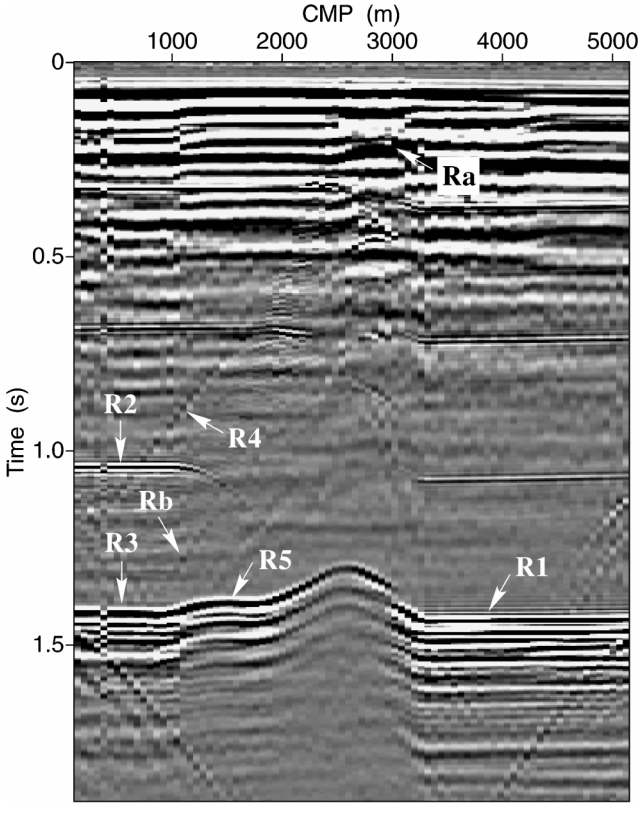

FIG. 2. Common-offset (200 m) time section of reflection data acquired over the model from Figure 1. The arrows mark the reflection events (R1–R5, Ra, and Rb) discussed in the text.

Reflection R1.—We begin with event R1 reflected from segment $[D_2D_3]$ beneath the isotropic homogeneous Plexiglass layer [Figure 3; see assumptions (1) and (3)]. The two-way zero-offset traveltime τ_{R1} and NMO velocity $V_{nmo,\,R1} = V_{iso}$ were picked from several semblance panels similar to the one shown in Figure 4a. Then we computed the mean values of the traveltimes and velocities over several common-midpoint (CMP) locations and obtained $\tau_{R1} = 1.437$ s and $V_{nmo,\,R1} = 2742$ m/s. The standard deviations attributable to picking inaccuracies, based on the spatial extent of the semblance maxima, were estimated at 0.004 s and 30 m/s (Figure 4a). The zero slope of reflection event R1 in Figure 2 indicates that segment $[D_2D_3]$ is horizontal. Its depth, which is supposed to be constant under the whole model according to assumption (4), is $z = z_{R1} = \tau_{R1} V_{iso}/2 = 1969 \pm 22$ m. Note that the computed depth z is somewhat greater than the correct value (1940 m) because it was determined using the traveltimes picked from the semblance maxima rather than from the actual first breaks. The notation $a = b \pm c$ means that the quantity a is equal to b with the error bar or standard deviation c. We estimated the

Table 2. For each reflection event in the left column, the table lists the attributes used in the inversion and the estimated model parameters.

Reflection event	Attributes used	Inverted parameters
R1	τ_{R1}, $V_{nmo,\,R1}$	$z(z_{R1})$, V_{iso}
R2	τ_{R2}, $V_{nmo,\,R2}$	z_{R2}
R3	τ_{R3}, $V_{nmo,\,R3}$	V_0, δ
R4	p_{R4}	ϕ
R5	τ_{R5}, $V_{nmo,\,R5}$	$z_\perp$, ϵ

Table 3. Comparison of the actual and inverted values of the velocities and anisotropic parameters.

Parameter	Actual	Inverted
V_{iso} (m/s)	2740	2742 ± 30
V_0 (m/s)	2925	2963 ± 157
ϵ	0.16	0.16 ± 0.06
δ	0.08	0.09 ± 0.06

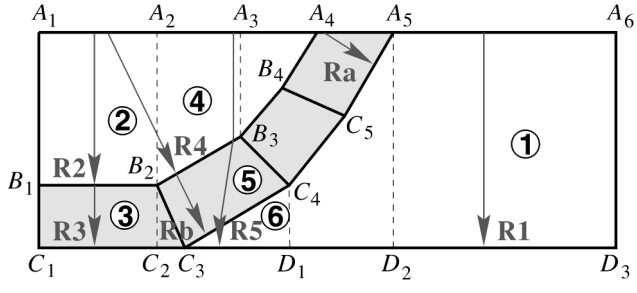

FIG. 3. Cartoon of the zero-offset rays R1–R5, Ra, and Rb. Numbers in the circles denote model blocks.

error bars for all intermediate quantities (not given in the text) and used them to evaluate the accuracy of the inverted model parameters.

Reflection R2.—Event R2 is similar to R1 because it also represents a reflection from the bottom of an isotropic homogeneous layer. Since the NMO velocity $V_{\text{nmo, R2}} = V_{\text{iso}} = 2750$ m/s (Figure 4b) practically coincides with $V_{\text{nmo, R1}}$ and the Plexiglass is supposed to homogeneous and isotropic, blocks 1 and 2 (Figure 3) have to be made of the same material. On the time section from Figure 2, reflection R2 can be seen as a horizontal event at the traveltime $\tau_{R2} = 1.05$ s; this implies that segment $[B_1 B_2]$ is horizontal. The estimated thickness of block 2 is $z_{R2} = \tau_{R2}\, V_{R2}/2 = 1444$ m.

Reflection R3.—Reflection R3, generated at the bottom of the horizontal block 3 (Figures 2 and 3), contains information about the NMO velocity V_{nmo} in the TTI layer. The symmetry axis in block 3 is vertical (i.e., the block has the VTI symmetry), and V_{nmo} is related to the symmetry-direction velocity V_0 as (Thomsen, 1986)

$$V_{\text{nmo}} = V_0\sqrt{1+2\delta}. \tag{1}$$

Since ray R3 propagates through a laterally homogeneous medium [assumption (1)], the interval NMO velocity can be found using the conventional Dix (1955) differentiation:

$$V_{\text{nmo}} = \sqrt{\frac{\tau_{R3} V^2_{\text{nmo, R3}} - \tau_{R2} V^2_{\text{nmo, R2}}}{\tau_{R3} - \tau_{R2}}} = 3192\text{m/s}, \tag{2}$$

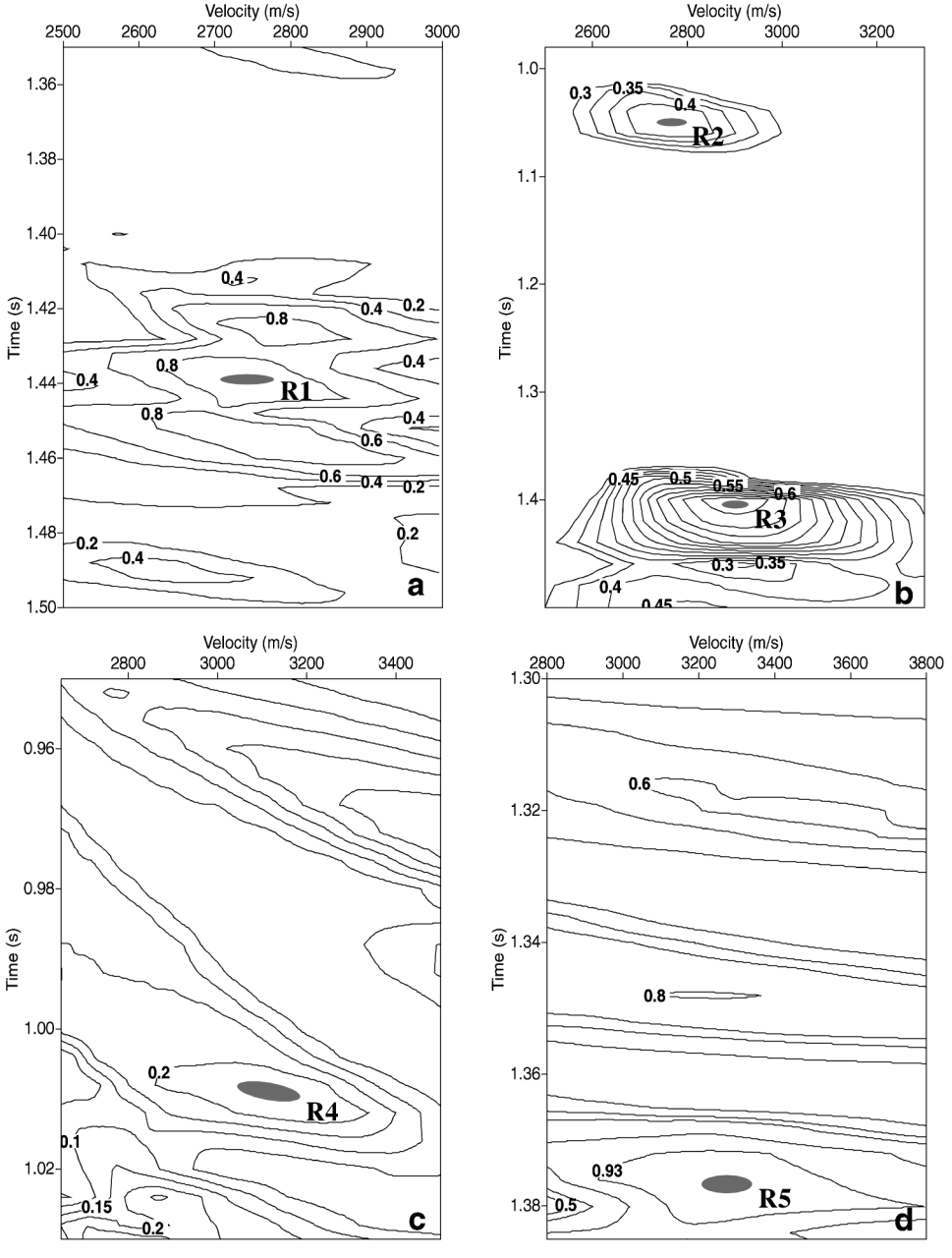

FIG. 4. Semblance contours at CMP locations 3780 m (a), 630 m (b), 680 m (c), and 1480 m (d). The gray areas mark the spatial dimensions of the semblance maxima used to pick the traveltimes and NMO velocities of reflection events R1–R5.

where $\tau_{R3} = 1.405$ s and $V_{nmo,\,R3} = 2870$ m/s are the measured zero-offset traveltime and NMO velocity for reflection R3 (Figure 4b). Under assumption (4), the depth of segment $[C_1C_2]$ is equal to that of segment $[D_2D_3]$: $z_{R3} = z_{R1} = 1969$ m. Therefore, we can compute the vertical velocity in block 3 as

$$V_0 = 2\frac{z_{R3} - z_{R2}}{\tau_{R3} - \tau_{R2}} = 2963\,\text{m/s}. \qquad (3)$$

Then, using equation (1), we find the anisotropic coefficient $\delta = 0.09$. As a result, conventional moveout analysis near the left edge of the model yields two parameters of the TTI layer: the symmetry-direction velocity V_0 and the coefficient δ. The other relevant anisotropic parameter, ϵ, still has to be found.

Reflection Ra.—To determine the parameter δ from horizontal events, we had to assume that the bottom interface is horizontal. An alternative way of estimating δ without such an assumption is to use the NMO velocity $V_{nmo,\,Ra}$ of the reflection from the dipping segment $[A_5C_5]$ (Ra in Figure 3). $V_{nmo,\,Ra}$ represents the following function of the velocities V_0, V_{nmo}, and the half-slope p_{Ra} of reflection Ra on the zero-offset section (Grechka and Tsvankin, 2000):

$$V_{nmo,\,Ra} = \frac{V_{nmo}}{\sqrt{1 - p_{Ra}^2\,V_0^2}}. \qquad (4)$$

With V_{nmo} already determined from horizontal events, equation (4) can be used to estimate V_0; then δ can be found from equation (1).

The NMO velocity of event Ra needs to be picked on a CMP gather within the relatively short segment $[A_4A_5]$. To avoid receiver locations outside this segment, offsets larger than approximately 500 m have to be muted. Even after the muting, however, accurate picking of the NMO velocity $V_{nmo,\,Ra}$ is practically impossible because of the absence of small offsets up to 200 m (Table 1) and relatively large (for such a shallow reflection) offset increment. The steep dip of interface $[A_5C_5]$ also contributes to the high uncertainty in the velocity picking. The above factors lead to strongly elongated semblance contours in Figure 5, which yield error bars for $V_{nmo,\,Ra}$ of at least 1000 m/s. Clearly, such an accuracy is inadequate for estimation of the anisotropic coefficients.

Reflections R4 and Rb.—Reflections R4 and Rb form parallel straight lines on the time section in Figure 2, which indicates that segments $[B_2B_3]$ and $[C_3C_4]$ of the TTI block 5 (Figure 3) are parallel to each other. Approximation of the picked zero-offset traveltimes of event R4 with a straight line (Figure 6) allows us to obtain the half-slope $p_{R4} = 1.82 \times 10^{-4}$ s/m. The NMO velocity $V_{nmo,\,R4} = 3120$ m/s corresponding to the semblance maximum in Figure 4c satisfies the isotropic relationship (within the error bars)

$$V_{nmo,\,R4} = \frac{V_{iso}}{\sqrt{1 - p_{R4}^2 V_{iso}^2}}. \qquad (5)$$

Although equation (5) is also valid for elliptically anisotropic media with the zero-dip NMO velocity V_{iso}, we use assumption (3) to identify blocks 2 and 4 (Figure 3) as part of the homogeneous isotropic section of the model. Then the dip ϕ of segment $[B_2B_3]$ is given by

$$\phi = \sin^{-1}(p_{R4}V_{iso}) = 29.8^\circ. \qquad (6)$$

Neither the traveltime τ_{Rb} nor the NMO velocity $V_{nmo,\,Rb}$ of event Rb could be picked because of its low amplitude (Figure 2). However, this does not hamper parameter estimation because both τ_{Rb} and $V_{nmo,\,Rb}$ are controlled by the model

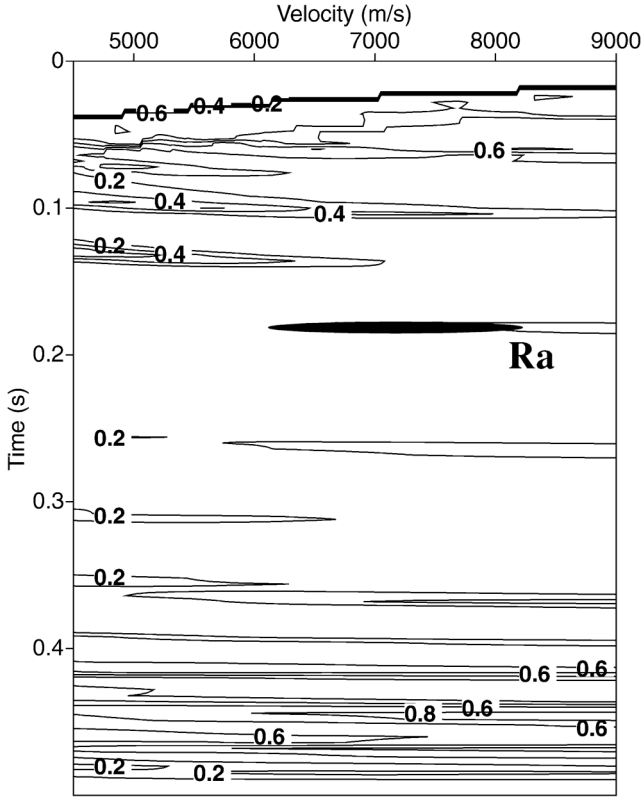

FIG. 5. Semblance contours for reflection Ra at CMP location 2810 m. The gray area indicates the range of possible moveout-velocity picks.

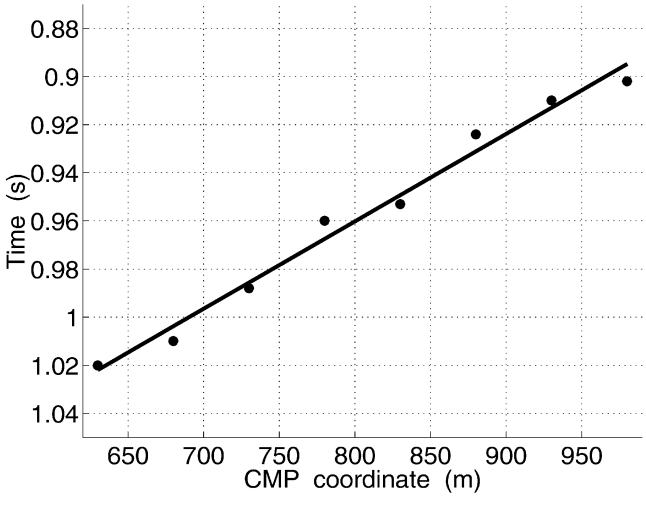

FIG. 6. Two-way zero-offset traveltimes (dots) for reflection R4 and their approximation with a straight line. The standard deviation of the picked traveltimes from the straight line is 0.006 s.

parameters that can be estimated from other reflections. For example, the traveltime τ_{Rb} could be used to obtain the thickness $z_\perp$ of block 5 (Figure 3) in the direction normal to interfaces $[B_2B_3]$ and $[C_3C_4]$. Since the symmetry axis is perpendicular to these interfaces [assumption (2)],

$$z_\perp = V_0\frac{\tau_{\mathrm{Rb}} - \tau_{\mathrm{R4}}}{2}. \tag{7}$$

Instead of using equation (7), however, we find the thickness $z_\perp$ from the traveltime of reflection R5 (see below).

Although it is natural to expect that the NMO velocity $V_{\mathrm{nmo,Rb}}$ contains information about the anisotropic parameter ϵ, this turns out not to be the case. The Dix-type averaging equation for tilted layers described by Grechka and Tsvankin (1999) leads to the following expression for $V_{\mathrm{nmo,\,Rb}}$:

$$V^2_{\mathrm{nmo,\,Rb}} = \frac{\tau_{\mathrm{R4}}V^2_{\mathrm{iso}} + (\tau_{\mathrm{Rb}} - \tau_{\mathrm{R4}})V^2_{\mathrm{nmo}}}{\tau_{\mathrm{Rb}}\cos^2\phi}, \tag{8}$$

where ϕ is the dip of interfaces $[B_2B_3]$ and $[C_3C_4]$ given by equation (6). Equation (8) shows that $V_{\mathrm{nmo,Rb}}$ depends on a single parameter of the TTI block—the NMO velocity V_{nmo} that has already been determined from the horizontal events. The same conclusion holds for the almost invisible reflection from segment $[C_4C_5]$ (Figure 3).

Reflection R5.—Both the thickness $z_\perp$ and the anisotropic coefficient ϵ can be found from the traveltime $\tau_{\mathrm{R5}} = 1.378$ s and the NMO velocity $V_{\mathrm{nmo,\,R5}} = 3250$ m/s of reflection R5 (Figures 4d and 7). Note than neither τ_{R5} nor $V_{\mathrm{nmo,\,R5}}$ depend on the CMP coordinate (Figure 2). This is possible only if segments $[B_2B_3]$ and $[C_3C_4]$ are parallel to each other (this has already been established by the analysis of events R4 and Rb) and the bottom interface $[C_3D_1]$ is horizontal. Consequently, the zero-offset ray R5 inside the isotropic blocks 4 and 6 has to be vertical (Figures 3 and 7). The zero-offset traveltime τ_{R5} of event R5 can be written as

$$\tau_{\mathrm{R5}} = \tau_{\mathrm{tti,\,R5}} + \tau_{\mathrm{iso,\,R5}}, \tag{9}$$

where $\tau_{\mathrm{tti,\,R5}}$ and $\tau_{\mathrm{iso,\,R5}}$ are the traveltimes inside the TTI and isotropic blocks, respectively. Using the relationships between the group(ray)-velocity vector and the horizontal (p) and vertical [$q = q(p)$] components of the slowness vector in the TTI block 5 (Grechka et al., 1999), we obtain

$$\tau_{\mathrm{tti,\,R5}} = 2z_\perp(q - pq')\frac{\cos\psi}{\cos(\phi+\psi)}, \tag{10}$$

$$\tau_{\mathrm{iso,\,R5}} = \frac{2}{V_{\mathrm{iso}}}\left(z - z_\perp\frac{\cos\psi}{\cos(\phi+\psi)}\right), \tag{11}$$

where

$$\psi = \tan^{-1}\left(\frac{dq}{dp}\right) \equiv \tan^{-1}q' \tag{12}$$

is the angle between the zero-offset ray and vertical inside block 5 (Figure 7). The slownesses p and q satisfy Snell's law at the top and bottom interfaces of block 5:

$$p = \left(q - \frac{1}{V_{\mathrm{iso}}}\right)\tan\phi. \tag{13}$$

In combination with the Christoffel equation in the TTI layer, Snell's law [equation (13)] can be used to obtain both slowness components for a given set of the TTI parameters and to compute the traveltime τ_{R5} from equation (9).

The NMO velocity $V_{\mathrm{nmo,\,R5}}$ provides a second equation for estimating $z_\perp$ and ϵ. The derivation of $V_{\mathrm{nmo,\,R5}}$, based on the results of Grechka and Tsvankin (1999), is omitted here because it essentially follows Appendix B of Le Stunff et al. (2001). The final expression has the form

$$V^2_{\mathrm{nmo,\,R5}} = \frac{1}{\tau_{\mathrm{R5}}}\left[\tau_{\mathrm{iso,\,R5}}V^2_{\mathrm{iso}} + \tau_{\mathrm{tti,\,R5}}\left(\frac{V_{\mathrm{tti,\,nmo}}(p)}{1 - q'\tan\phi}\right)^2\right], \tag{14}$$

where

$$V^2_{\mathrm{tti,\,nmo}}(p) = \frac{d^2q/dp^2}{pq' - q} \tag{15}$$

is the interval NMO velocity within the TTI block evaluated for the horizontal slowness component p of the zero-offset ray (Grechka et al., 1999).

After picking τ_{R5} and $V_{\mathrm{nmo,\,R5}}$ from the semblance panel in Figure 4d, we perform nonlinear inversion of equations (9) and (14) and obtain accurate estimates of $z_\perp = 594$ m and $\epsilon = 0.16$. Complete results of the parameter-estimation procedure are summarized in Table 3.

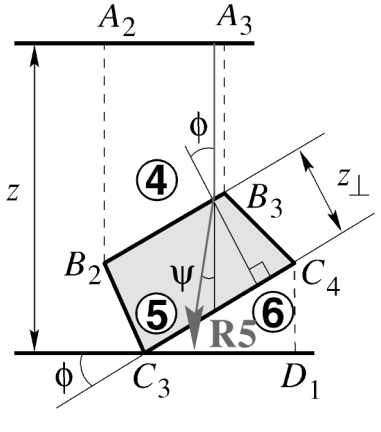

FIG. 7. Notation associated with the zero-offset ray of reflection R5 from the horizontal interface $[C_3D_1]$ below the TTI block 5.

DISCUSSION AND CONCLUSIONS

The presence of transverse isotropy with a tilted symmetry axis (TTI media) causes significant distortions in the results of conventional velocity analysis and imaging in overthrust areas. While migration algorithms can be extended to TTI models in a relatively straightforward way, estimating the anisotropic parameters needed to build the velocity model is a much more difficult task. The structural setting of overthrust areas is characterized by steep dips and substantial lateral heterogeneity, which further complicates the recovery of the anisotropic velocity field from surface reflection data.

Still, for models without a substantial velocity variation within layers or blocks, it may be possible to invert P-wave reflection traveltimes acquired in the dip direction of the structure for all relevant parameters of TTI media. Here, we used the physical-modeling data of Leslie and Lawton (1996) to determine the thickness, symmetry-direction velocity V_0, and the anisotropic coefficients ϵ and δ of a bending TI layer. This

model was built to simulate the distinctive features of typical reflection data acquired over TTI shale layers in the Alberta Foothills. Two important constraints on the TTI model were provided by the geologically justified assumptions that the symmetry axis is orthogonal to the bedding and the TTI layer is homogeneous. Another, more arbitrary assumption used in the inversion procedure was that the bottom of the model is horizontal. The depth of the bottom reflector under the TTI layer, however, could have been determined from the data had the acquisition geometry allowed us to process reflections from steeply dipping interfaces in the shallow portion of the model.

While estimation of the symmetry-direction velocity V_0 and the coefficient δ using horizontal reflection events and the depth of the bottom interface was based on well-known techniques, obtaining the parameter ϵ represented the most nontrivial part of the inversion procedure. As follows from the analytic description of normal moveout in laterally heterogeneous media given by Grechka and Tsvankin (1999), information about ϵ is contained only in the NMO velocity and zero-offset traveltime of arrivals which cross the dipping TTI blocks and reflect from the bottom of the model (Figures 3 and 7). The inversion using one of these reflection events allowed us to determine not only the value of ϵ, but also the thickness of the dipping TTI block. Thus, under the assumptions listed above, *P*-wave reflection traveltimes proved to be sufficient to reconstruct the TTI model in the depth domain.

Semianalytic inversion methods based on moveout velocities may become inaccurate for more complicated media, but in most cases they can still be used to build an initial model for migration velocity analysis. The feasibility of anisotropic parameter estimation in TTI media strongly depends on the degree of structural complexity and the range of propagation directions covered by the zero-offset reflected rays. As long as the lateral variation in the elastic parameters is not substantial, the presence of bending TTI layers with variable dips may actually help in the inversion by generating reflected rays that cross the TTI blocks at different angles with the symmetry axis. In general, the results of this work show that the issue of ambiguity in the parameter estimation has to be carefully addressed for each specific TTI model.

One of our objectives was to estimate the confidence intervals for all inverted quantities. These error bars were obtained by visually inspecting the spatial extent of the semblance maxima used to pick the NMO velocities and zero-offset traveltimes. Although this approach is somewhat subjective, it still provides useful information about the uncertainties in the traveltime inversion for anisotropic media. It should be mentioned that the accuracy in velocity picking can be substantially increased by upgrading the acquisition geometry (i.e., recording small offsets, reducing the receiver spacing etc.).

ACKNOWLEDGMENTS

We thank Don Lawton (University of Calgary) for providing the physical-modeling data and discussing various aspects of the imaging problem in TTI media. We are grateful to members of the A(nisotropy)-Team of the Center for Wave Phenomena (CWP), Colorado School of Mines, for helpful suggestions. This work was supported by the members of the Consortium Project on Seismic Inverse Methods for Complex Structures at CWP and by the United States Department of Energy (award #DE-FG03-98ER14908). I. Tsvankin was also supported by the Shell Faculty Career Initiation Grant.

REFERENCES

Alkhalifah, T., and Tsvankin, I., 1995, Velocity analysis in transversely isotropic media: Geophysics, **60**, 1550–1566.

Cheadle, S. P., Brown, R. J., and Lawton, D. C., 1991, Orthorhombic anisotropy: A physical seismic modeling study: Geophysics, **56**, 1603–1613.

Dix, C. H., 1955, Seismic velocities from surface measurements: Geophysics, **20**, 68–86.

Grechka, V., 1998, Transverse isotropy versus lateral heterogeneity in the inversion of *P*-wave reflection traveltimes: Geophysics, **63**, 204–212.

Grechka, V., and Tsvankin, I., 1999, NMO surfaces and Dix-type formulae in heterogeneous anisotropic media: 69th Ann. Internat. Mtg., Soc. Expl. Geophys., Expanded Abstracts, 1612–1615.

——— 2000, Inversion of azimuthally dependent NMO velocity in transversely isotropic media with a tilted axis of symmetry: Geophysics, **65**, 232–246.

Grechka, V., Tsvankin, I., and Cohen, J. K., 1999, Generalized Dix equation and analytic treatment of normal-moveout velocity for anisotropic media: Geophys. Prosp., **47**, 117–148.

Isaac, J. H., and Lawton, D. C., 1999, Image mispositioning due to dipping TI media: A physical seismic modeling study: Geophysics, **64**, 1230–1238.

Leslie, J. M., and Lawton, D. C., 1996, Structural imaging below dipping anisotropic layers: Predictions from seismic modeling: 66th Ann. Internat. Mtg., Soc. Expl. Geophys., Expanded Abstracts, 719–722.

——— 1998, Anisotropic pre-stack depth migration: The Recorder, **23**, No. 10, 23–36.

Le Stunff, Y., Grechka, V., and Tsvankin, I., 2001, Depth-domain velocity analysis in VTI media using surface *P*-wave data: Is it feasible?: Geophysics, **66**, pp. 897–903, this issue.

Levin, F. K., 1979, Seismic velocities in transversely isotropic media: Geophysics, **44**, 918–936.

Thomsen, L., 1986, Weak elastic anisotropy: Geophysics, **51**, 1954–1966.

Tsvankin, I., 1996, *P*-wave signatures and notation for transversely isotropic media: An overview: Geophysics, **61**, 467–483.

——— 1997, Moveout analysis for transversely isotropic media with a tilted symmetry axis: Geophys. Prosp., **45**, 479–512.

Vestrum, R. W., Lawton, D. C., and Schmid, R., 1999, Imaging structures below dipping TI media: Geophysics, **64**, 1239–1246.